

## Surface characterization of EPD coating on AZ91 Mg alloy produced by powder metallurgy

İbrahim Aydın<sup>a</sup>, Ali İhsan Bahçepinar<sup>a,✉</sup>, Canser Gül<sup>b</sup>

<sup>a</sup>Manisa Celal Bayar University, Vocational School of Technical Sciences, Machinery and Metal Technologies Department, Manisa

<sup>b</sup>Manisa Celal Bayar University, Engineering Faculty, Department of Metallurgical and Materials Engineering, Manisa

(✉Corresponding author: [ali.bahcepinar@cbu.edu.tr](mailto:ali.bahcepinar@cbu.edu.tr))

Submitted: 27 February 2020; Accepted: 12 August 2020; Available On-line: 9 October 2020

**ABSTRACT:** Intense implants which are used widely in biomedical applications such as Ti and its alloys and 316 L stainless steel can harm the surrounding tissues, hence may also cause infection. In order to eliminate this risk, it is necessary to produce new generation implant materials that are lighter than their existing biomaterials for use in biomedical applications and whose mechanical properties and structure are close to bone. In this study AZ91 Mg alloy implant material is created by using powder metallurgy method. In addition, in order to improve the bio-compatibility and bio-activity, the generated implant material was also coated with hydroxyapatite (HA) which is known as a ceramic based biomaterial. In this study, AZ91 Mg alloy is created by using powder metallurgy method. HA coating was applied to the alloy surface using the electrophoretic deposition method. The surface properties and corrosion resistance of the coatings made were examined. The applied voltage values in the coating process were determined as 100, 150, 200 and 250 V, the time parameter was stabilized as 2 minutes. HA, ethanol, polyvinyl alcohol (PVA), N, N-Dimethylformamide chemicals were used to prepare the coating solution. At the end of the study, microstructures of the coatings were examined by using scanning electron microscopy (SEM) and elemental analyzes (EDS) of the coating surfaces were performed. The X-ray diffraction method (XRD) was used to determine the phases of the coatings and its concentration. Coating thickness and surface roughness values were also determined. Corrosion behavior of coated samples was determined by potentiodynamic electrochemical potential corrosion test in artificial body fluid.

**KEYWORDS:** AZ91 Mg alloy; Coating; Electrophoretic deposition (EPD); Hydroxyapatite (HA); Powder Metallurgy (P/M)

**Citation/Citar como:** Aydın, İ.; Bahçepinar, A.İ.; Gül, C. (2020). "Surface characterization of EPD coating on AZ91 Mg alloy produced by powder metallurgy". *Rev. Metal.* 56(3): e176. <https://doi.org/10.3989/revmetalm.176>

**RESUMEN:** *Caracterización de la superficie de un recubrimiento EPD sobre la aleación de Mg AZ91 obtenida mediante Pulvimetalurgia.* Los implantes habituales en aplicaciones biomédicas como el Ti y sus aleaciones y el acero inoxidable 316L pueden dañar los tejidos circundantes, ocasionando infecciones. Para evitar este riesgo, es necesario producir materiales de implantes de nueva generación que sean más ligeros que los biomateriales existentes, en los que las propiedades mecánicas y estructura sean similares al hueso. En este estudio, el material de implante de aleación de Mg AZ91 se obtiene mediante un procedimiento pulvimetalúrgico. Adicionalmente, para mejorar la biocompatibilidad y bioactividad, el material de implante obtenido se recubrió con hidroxapatita (HA), conocido como biomaterial de base cerámica. Se aplicó un revestimiento de HA a la superficie de la aleación utilizando el método de deposición electroforética. Se examinaron las propiedades superficiales y la resistencia a la corrosión. Los valores de voltaje aplicados en el proceso de recubrimiento fueron 100, 150, 200 y 250 V, durante un tiempo de 2 min. Se utilizaron productos químicos de HA, etanol, alcohol polivinílico (PVA), N, N-dimetilformamida para preparar la solución de revestimiento. Se analizaron las microestructuras de los recubrimientos mediante microscopía electrónica de barrido (SEM) y se realizaron análisis elementales (EDS) de las superficies del recubrimiento. Se utilizó el método de difracción de rayos X (XRD) para determinar las fases de los recubrimientos y su concentración. Finalmente, se determinaron los valores de espesor del revestimiento y la rugosidad superficial. El comportamiento frente a la corrosión se determinó mediante la medida de potencial de corrosión, utilizando como electrolito un fluido corporal artificial.

**PALABRAS CLAVE:** Aleación AZ91 Mg; Deposición electroforética (EPD); Hidroxapatita (HA); Metalurgia de polvos (P/M); Revestimiento

**ORCID ID:** İbrahim Aydın (<https://orcid.org/0000-0002-6281-4902>); Ali İhsan Bahçepinar (<https://orcid.org/0000-0002-9744-0146>); Canser Gül (<https://orcid.org/0000-0002-1339-936X>)

**Copyright:** © 2020 CSIC. This is an open-access article distributed under the terms of the Creative Commons Attribution 4.0 International (CC BY 4.0) License.

## 1. INTRODUCTION

Mg alloys are using in many fields such as automobile or space industries. AZ series Mg alloys such as AZ31, AZ80, and AZ91 are studied frequently for their biocompatibility, lightness and their relative corrosion resistance comparing to the other mg alloys (Agarwal *et al.*, 2016). These properties of Mg alloys raise the question of whether it can be used as a permanent implant in recent years due to its mechanical properties close to the natural bone ( $1.8\text{--}2.1\text{ g}\cdot\text{cm}^{-3}$ ) (Brandes and Brook, 1998; Bandyopadhyay *et al.*, 2010; Ivanova *et al.*, 2014). Mg alloys are lightweight metals with density ranging from  $1.74$  to  $2.0\text{ g}\cdot\text{cm}^{-3}$ , that is much lighter than titanium alloys ( $4.4\text{--}4.5\text{ g}\cdot\text{cm}^{-3}$ ), Co-Cr alloys ( $4.5\text{--}8.3\text{ g}\cdot\text{cm}^{-3}$ ) (Ivanova *et al.*, 2014; Zhang *et al.*, 2015).

AZ series alloys mostly consist of  $\alpha$ -grains and secondary  $\beta$ -phases. These secondary phases such as Mg<sub>17</sub>Al<sub>12</sub> precipitate at the grain boundaries and cause the presence of localized galvanic couples between  $\alpha$ -grains and secondary phases. But this mechanism not the only reason for the fast degradation of magnesium alloys (Sahoo and Panigrahi, 2016; Wang *et al.*, 2017; Chowdary *et al.*, 2018). Pitting corrosion is also affecting the degradation especially in the presence of chloride ions (Tahmasebifar *et al.*, 2016). The human body is a very harsh environment that contains many ions such as chlorine and so on (Salman *et al.*, 2013). Therefore, various studies have been carried out to prevent this degradation in mg alloys.

Various studies were carried out to increase the bioactivity, corrosion or wear resistance of Mg and its alloys (Chen *et al.*, 2008; Salman *et al.*, 2013; Esmaily *et al.*, 2016). Some of them were designed to provide various properties using reinforcing elements (Esmaily *et al.*, 2016), while others aimed at forming an oxide layer on the surface using heat treatments (Niu *et al.*, 2016; Chen *et al.*, 2017). Coatings were made to ensure that similar properties are also available (Brusciotti *et al.*, 2013; Rojaee *et al.*, 2013).

Coatings were made to ensure that Hydroxyapatite (HA) is a calcium phosphate product, which is the essential component of the human bone, having a high bio-activity and bio-compatibility (Bogdanoviciene *et al.*, 2006; Javidi *et al.*, 2008; Iqbal *et al.*, 2012; Morteza, 2018a). However, due to its low mechanical properties, it is not appropriate to be directly used in human body (Miranda *et al.*, 2019). Its application of being coated on the surfaces of the metallic biomaterials having high mechanical properties supports its usage in human body more (Javidi *et al.*, 2008; Iqbal *et al.*, 2012; Luo *et al.*, 2018). Also HA has a significant place in biomaterials due to the fact of supporting the bone growth (Javidi *et al.*, 2008; Miranda *et al.*, 2019).

There are various methods like sol-gel, biomimetic method, electrochemical precipitation, plasma spraying and electrophoretic deposition (EPD) for the HA coating of metallic implants (Abdeltawab *et al.*, 2011; Iqbal *et al.*, 2012; Bartmanski *et al.*, 2018). Among these the one which has the highest potential of usage in industry is EPD method. With this method, the coating process occurs with the deposition of the charged particles which are spread in an electrolytic suspension on the counter electrode moving by the effect of electrical force (Pang *et al.*, 2009; Sreekanth and Rameshbabu, 2012; Drevet *et al.*, 2016; Morteza, 2018b). EPD method, which is preferred in industry, is a simple method due to its advantages like coating thickness control, creating homogeneous coatings, low equipment cost, coating materials with complex structures (Iqbal *et al.*, 2012; Morteza and Shahrabi, 2013; Khalili *et al.*, 2016; Morteza, 2018b; Sabzi *et al.*, 2018). The biggest disadvantage of EPD method is that it needs sintering at high temperatures (Khalili *et al.*, 2016). Alcohols are used as solvents in the preparation of EPD suspensions. The reason is that alcohols act as proton donors. Ethanol in the alcohols group is an easy-to-find solvent commonly used in the EPD method (Abdeltawab *et al.*, 2011).

## 2. MATERIALS AND METHODS

### 2.1. Implant material selection

AZ91 Mg alloy powders containing the components given in Table 1 were hot compacted by hot isostatic pressing (HIP) at 275 MPa and 325 °C for 1 h for substrate production. Powders, which have particle size distribution given in Table 2, were selected because of their commercial availability and frequently used in biomaterial applications. The density values of the samples reached up to 98.6% of the theoretical density, according to the Archimedes' Principle. Produced AZ91 Mg alloy was cut in to  $30\times 10\times 2\text{ mm}^3$  dimensions.

TABLE 1. The chemical components of AZ91 Powders

	Al	Zn	Mn	Other	Mg
AZ91D	8.80	0.71	0.19	Max 0.033	Balance

TABLE 2. Particle Dimension Distribution

Distribution	Size ( $\mu\text{m}$ )
d10	52.3
d50	179.2
d90	605.1

AZ91 Mg alloy, which we used in the study as a base material, was created with powder metallurgy method as an alternative to present biomedical materials. Besides it's a candidate of new generation implant materials due to the fact that it's lightweight and it has a structure closer to bone's.

## 2.2. The preparation of the coating

In the study, AZ91 Mg alloyed implant materials were rubbed by using SiC emery paper and they were washed with detergent water. Then they were cleansed in ultrasonic bath with wash of pure water for 30 min, with wash of ethyl alcohol 30 min and with wash of pure water 30 min respectively. Finally, they were made ready for the coating process by having been dried in the oven at 25 °C.

In electrophoretic deposition process ethanol was used at a purity of 99.8%. By having added 1 g of HA and 1 g of PVA and 10 ml of N,N-Dimethylformamide (Sigma-Aldrich) in 100 ml of ethanol they were mixed in a magnetic mixer for 30 min and the homogeneous diffusion of HA powders was provided in a teflon beaker. In order to provide suspension stability, the Ph value was set as 4 by using HNO<sub>3</sub> and NaOH.

For the coating process AZ91 Mg alloys were placed as anode and cathode by making the surfaces face to each other to be coated. The distance between them was set as 10 mm. They were dipped in stable suspension prepared in Teflon beaker and were connected to DC power supply (Bio RAD Powerpac Basic). In order to examine the effect of

the voltage which was applied at a constant period to the coating properties, the voltage effect period was kept at a constant value of 2 min, the voltage values were set as 100, 150, 200 and 250 V. The coating operations were performed at these parameters.

In order to increase the bonding strength of the coatings which were gained, the coatings were kept at room temperature for 24 hours, then they were heated up to 400 °C at a heating speed of 2 °C·min<sup>-1</sup>. They were left to be cooled by having been kept at 400 °C for 1 hour.

## 3. RESULTS

### 3.1. SEM-EDX results

The microstructure examination analyzes of the coated samples were performed by using QUANTA 250 FEG model scanning electron microscope. 5000x images of the results gained on the microstructural examinations which were performed on SEM are given on Fig. 1. When SEM images are examined it is seen that the HA structure successfully occurred on the surface. At 250 V it was seen that there occurred deep holes and fractures in the structure.

The elemental component of the structures and the coated samples were determined by using EDX detector on QUANTA 250 FEG model scanning electron microscope. The EDX results of the coatings created at different voltage periods are given on Fig. 2. When the results were examined, it was

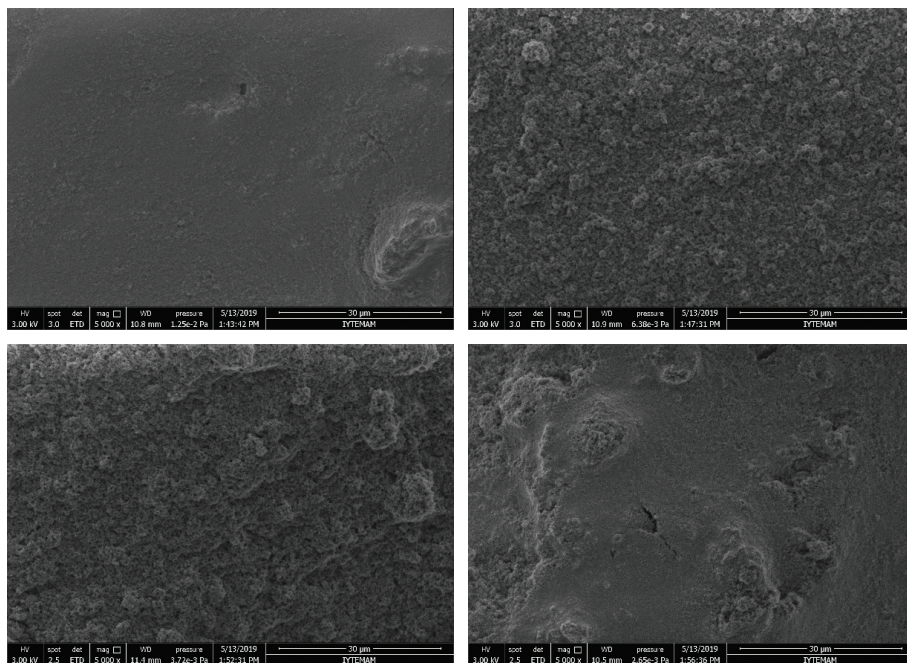


FIGURE 1. SEM images of HA coated AZ91 Mg alloys: (a) 100 V/120 s, (b) 150 V/120 s, (c) 200 V/120 s, and (d) 250 V/120 s.

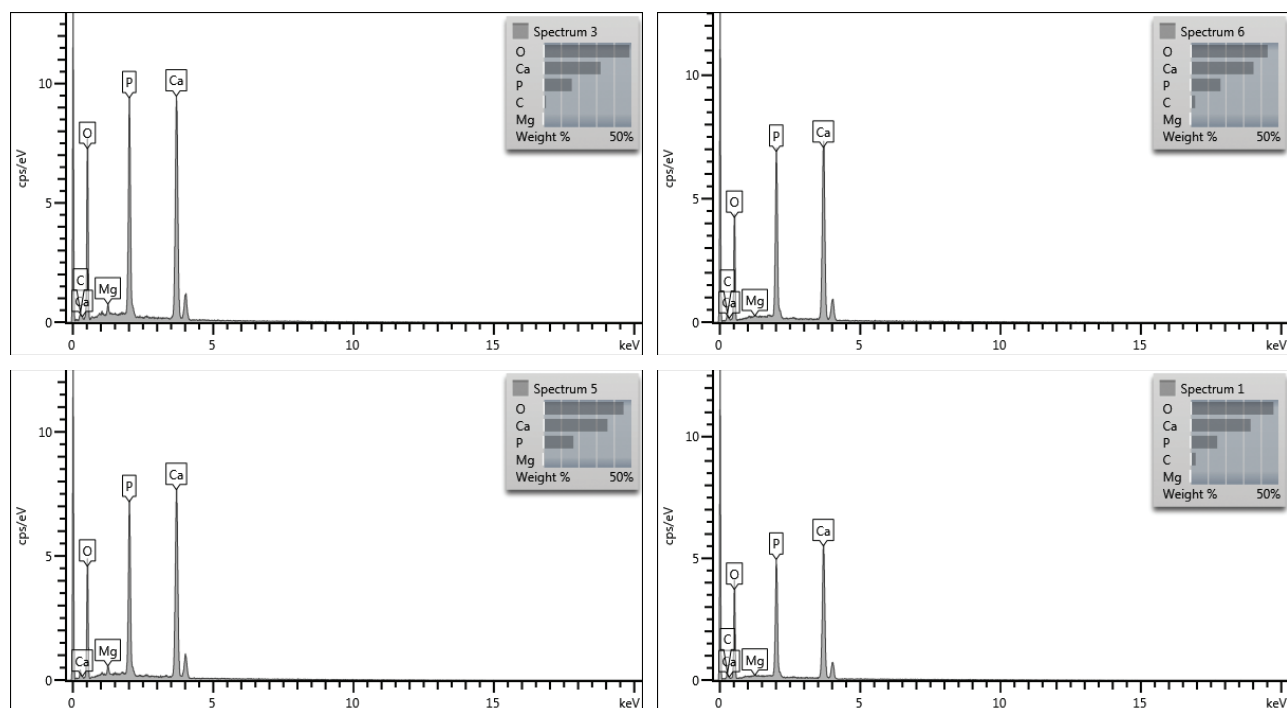


FIGURE 2. EDS results of HA coated AZ91 Mg alloys: (a) 100V/120s, (b) 150V/120s, (c) 200V/120s, and (d) 250V/120s.

TABLE 3. Ca/P rate for different voltage values

Voltage	100 V	150 V	200 V	250 V
Ca/P	1.59	1.63	1.66	1.72

detected that a calcium phosphate structure had occurred on all coatings. Besides the Ca/P rates calculated through these results for each parameter are given on Table 3.

### 3.2. XRD results

In order to determine the phases which the coated samples contained and the concentration of these phases, PHILIPS X'PERT PRO X radiation diffraction device (XRD) was used. Figure 3 shows the results of the XRD tests. According to the test results, the HA crystals occurred at peak points of 25.7182°, 28.7945°, 31.6402°, 32.0520°, 32.6648°, 32.7802°, 33.8369°, 33.926°, 39.6934°, 46.2985°, 49.3822° and 70.7743° respectively.

### 3.3. Coating thickness results

The thickness of HA coatings which were performed by using electrophoretic deposition method, was evaluated with ElektroPhysik MiniTest 730/Sensor FN 1.5 HD trademark device in terms of micrometer. The averages of the results were taken

by performing evaluations on each coating surface 5 times. For each coating gained at 100, 150, 200 and 250 V values at a deposition period of 2 min five evaluations were performed and averages of the results were taken. The average values of the coating thicknesses gained from the evaluation results are given on Table 4.

### 3.4. Surface roughness results

For the determination of the surface roughness values of the samples gained by the result of the coatings, Roughness Tester PCE-RT 1200 model device was used. On the coating the evaluation range was determined as 12.5 mm and the evaluation speed was determined as 0.5 mm·s<sup>-1</sup>, the results were gained in terms of micrometer. Surface roughness was measured 5 times in each sample coated with 100, 150, 200 and 250 V for 2 min and averages of the results were taken. The average roughness values gained by the evaluation results are given on Table 5.

### 3.5. Corrosion test results

The corrosion tests of the samples were carried out in simulated body fluid (SBF) prepared as an electrolyte. The chemicals used in the SBF preparation were given in Table 6. The first five chemicals were dissolved in 700 ml deionized water respectively. After the fifth chemical added, 15 ml of 1M

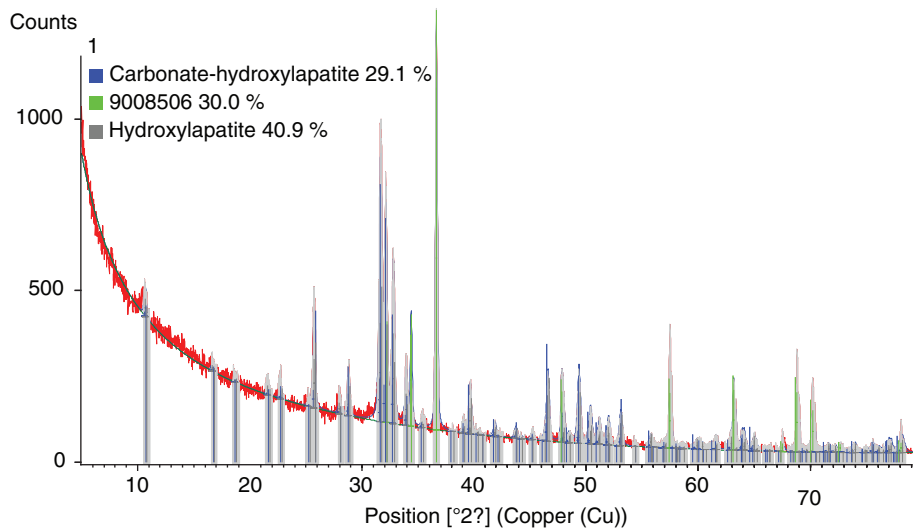


FIGURE 3. XRD Analysis Results.

TABLE 4. The average thicknesses of HA coatings

Voltage	100 V	150 V	200 V	250 V
Coating Thicknesses (µm)	5.86 ± 0.066	7.73 ± 0.143	9.72 ± 0.106	12.11 ± 0.178

TABLE 5. The average roughnesses of HA coatings

Voltage	100 V	150 V	200 V	250 V
Surface Roughnesses (Ra)(µm)	1.18 ± 0.072	1.95 ± 0.152	2.26 ± 0.131	2.83 ± 0.187

TABLE 6. Chemical composition for 1 liter SBF solution (Pasinli *et al.*, 2010)

Chemical	g·L <sup>-1</sup>
NaCl	6.547
NaHCO <sub>3</sub>	2.268
KCl	0.378
Na <sub>2</sub> HPO <sub>4</sub> ·2H <sub>2</sub> O	0.178
MgCl <sub>2</sub> ·6H <sub>2</sub> O	0.305
CaCl <sub>2</sub> ·2H <sub>2</sub> O	0.368
Na <sub>2</sub> SO <sub>4</sub>	0.071
(CH <sub>2</sub> OH) <sub>3</sub> CNH <sub>2</sub>	6.057

HCl solution was added. Subsequently, the other chemicals were added sequentially. After dissolving the final chemical, the temperature was increased to 37 °C, body temperature, adjusted to pH 7.4 using 1M HCl solution. Then, deionized water was added to complete the solution volume to 1 L.

Corrosion tests were carried out by using Metrohm potentiostat-galvanostat corrosion device

with three electrode system. A saturated calomel electrode (SCE) was used as a reference electrode, graphite electrode was used as a counter electrode and insulated sample outside the specific surface area was used as a working electrode. The open circuit potential of 120 s was measured in the prepared SBF solution and then corrosion tests were performed. Potential in the range of -250 mV and 250 mV was applied to the samples with 1 mV·s<sup>-1</sup>. Electrochemical potential curves of the samples obtained in the measurement results was given in Fig. 4 and corrosion rates was given in Fig. 5.

#### 4. DISCUSSION

Aydın *et al.* (2019) observed HA crystals at peak points of 2 Theta= 26.0078°, 28.1945°, 32.2494°, 34.1778°, 39.9130°, 48.1571° and 50.5511° on XRD results of the coatings which they gained in the HA coating process, which they had conducted on the surface of Ti6Al7Nb alloy with EPD method. Kumar *et al.* (2016) observed HA crystals at peak points of 2 Theta= 26.06°, 31.62° on XRD results of the coatings which they gained in the HA coating

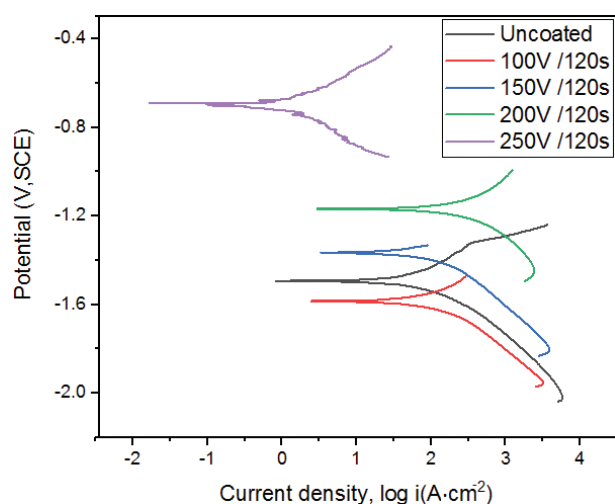


FIGURE 4. Electrochemical potential curves of samples.

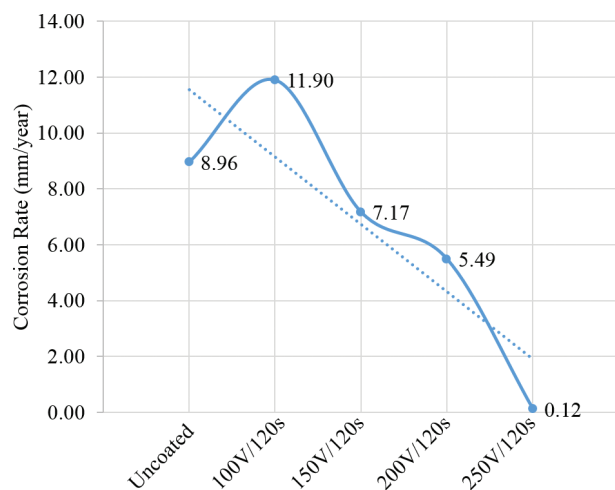


FIGURE 5. Corrosion rates of samples.

process, which they had conducted on the surface of Mg-3Zn alloy at  $20 \text{ V}\cdot\text{cm}^{-1}$  for 10 min with EPD method. Iqbal *et al.* (2012) observed HA crystals at peak points of  $25.91^\circ$ ,  $28.94^\circ$ ,  $32.2494^\circ$ ,  $31.78^\circ$ ,  $32.19^\circ$ ,  $32.93^\circ$ ,  $34.10^\circ$ ,  $39.80^\circ$ ,  $46.71^\circ$ ,  $49.49^\circ$  in the coating process they had conducted on 316L stainless steel.

By the results of conducted evaluations, when the coating thickness values are examined, it's seen that surface roughness value increases due to the increasing voltage value. Aydın *et al.* (2019) determined the coating thicknesses as  $4.38 \mu\text{m}$ ,  $5.43 \mu\text{m}$ ,  $7.60 \mu\text{m}$ ,  $9.42 \mu\text{m}$  respectively on the HA coatings, which they had performed on Ti6Al7Nb alloy by applying 50V,100V,150V,200V at a deposition period of 1 minute. Kwork *et al.* (2009) determined the coating thickness approximately as  $10 \mu\text{m}$  in the HA coating process, which they had performed on Ti6Al4V bases at 200 V for 3 minutes. Bartmanski

*et al.* (2018) conducted a hydroxyapatite coating process on Ti13Zr13Nb bases in the solution, which they had prepared by using 0.5 g of hydroxyapatite in 100 ml of ethanol, at 50 V for 1 min and they determined the coating thickness approximately as  $29.35 \mu\text{m}$ . Dudek and Goryczka (2016) conducted a HA coating process on NiTi shape memory alloy at different voltages and periods, they determined the coating thicknesses as  $2.6 \mu\text{m}$  at 80V in 1 min,  $2.8 \mu\text{m}$  at 100 V in 1 min,  $4.2 \mu\text{m}$  at 80V in 2 min.

By the results of conducted evaluations, when the roughness values are examined, it's seen that surface roughness value increases due to the increasing voltage value. Aydın *et al.* (2019) evaluated the surface roughness values as  $0.818 \mu\text{m}$ ,  $1.055 \mu\text{m}$ ,  $1.552 \mu\text{m}$ ,  $1.673 \mu\text{m}$  respectively on the HA coatings, which they had performed on Ti6Al7Nb alloy by applying 50 V,100 V,150 V and 200 V. Bartmanski *et al.* (2018) evaluated the surface roughness value as  $1.26 \mu\text{m}$  by the result of the coating process on Ti13Zr13Nb bases in the solution, which they had prepared by using 0.5 g of hydroxyapatite in 100 ml of ethanol at 50 V for 1 min. Javidi *et al.* (2008) gained coatings at different voltages and periods in the HA coating process which they had performed on 316L stainless steel, they evaluated the surface roughness value as  $1.8 \mu\text{m}$  on the coating they had gained at 90 V and at a deposition period of 180 s. Besides they determined that surface roughness increased within the increasing voltage.

Potential-current density graphs show that the potential values towards more positive values indicate higher corrosion resistance of these samples (Perez, 2004). In this case, it can be said roughly that the 100V/120s coated sample has the lowest corrosion resistance and the 250V/120s coated sample has the highest corrosion resistance. When the corrosion rates of the samples were examined, it was found that the results were consistent with their potential values. The coating thickness increased with increasing potential used in the coating process, and corrosion resistance of the samples tended to increase with increasing coating thickness.

When SEM images were examined in Fig. 1, it was observed that there were porosities on the sample surface coated with 250V/120s. However, the corrosion performances were examined; it was found that this sample was more resistant to corrosion than the others. In fact, it is expected that the corrosion resistance of such a porosity-containing material will be reduced. The higher corrosion resistance of this sample can be attributed to deep cavities seen do not reach the substrate material. When the Tafel curve of this sample was examined, it was found to be rougher than other curves. These sharp changes in the potential flow graph are associated with pitting corrosion (Perez, 2004). However, the findings support that the gaps were closed to the substrate surface. Furthermore, this

is not only related to voids in the coating layer. The measured surface roughness values also contain information on corrosion behavior. In their study, Alvarez *et al.* (2010) emphasized that increased surface roughness prevents pitting corrosion and this may prevent the decrease in corrosion potentials (Alvarez *et al.*, 2010).

The corrosion resistance of the uncoated sample was surprisingly not the lowest. The corrosion performance of the 100V/120s coated sample was lower than the uncoated AZ91D sample, which may be due to insufficient coating thickness. The presence of pits open to the bottom in small amounts of coated samples may decrease the corrosion resistance as it increases the ion concentration at these points (Song, 2011).

## 5. CONCLUSIONS

- In this study, the creation of a new generation implant material, AZ91 Mg, was produced by using powder metallurgy method, the HA coating process was applied on the surface of the produced material by using electrophoretic deposition method.
- At the end of the study, when SEM images were examined the homogeneous coatings were gained at all parameters. Also it is seen that the surface roughness value increased due to the increasing voltage. At 250 V it is seen that there occurred deep holes and fractures in the structure.
- By the EDX analysis results belonging to the HA coatings, which were gained at different voltage values, when the Ca/P rate, which was evaluated for each parameter, was examined, it was determined as 1.59 at 100 V, 1.63 at 150 V, 1.66 at 200 V, 1.72 at 250 V. It was seen that the value of 1.67 as known as ideal Ca/P rate was approached at all parameters. It was seen that the value of 1.67 as known as ideal Ca/P rate was approached in the coated sample at 200 V/120s.
- When the coating thickness results were examined, the lowest coating thickness was evaluated as 5.86  $\mu\text{m}$  at 100V and the highest coating thickness was evaluated as 12.11  $\mu\text{m}$  at 250 V. It was also determined that the coating thickness increased within the increasing voltage.
- When the surface roughness results were examined, the lowest surface roughness was evaluated as 1.18  $\mu\text{m}$  at 100V and the highest surface roughness was evaluated as 2.83  $\mu\text{m}$  at 250 V. It was determined that the surface roughness increased within the increasing voltage.
- When the corrosion test results were examined, it was determined that the 250 V coated sample had the highest corrosion resistance. The corrosion resistance of the 100 V coated sample was determined to be the lowest.
- At the end of the study, when the results of the mechanical, metallographic and corrosion tests performed were evaluated, the samples coated at 200V/120s were chosen as the most ideal parameters because they are close to the ideal Ca / P ratio and have high corrosion resistance. Although the samples covered with 250V/120s show higher corrosion resistance, At 250 V it is seen that there occurred deep holes and fractures in the structure.

## REFERENCES

- Abdeltawab, A.A., Shoeib, M.A., Mohamed, S.G. (2011). Electrophoretic deposition of hydroxyapatite coatings on titanium from dimethylformamide suspensions. *Surf. Coat. Tech.* 206 (1), 43–50. <https://doi.org/10.1016/j.surfcoat.2011.06.034>.
- Alvarez, R.B., Martin, H.J., Horstemeyer, M.F., Chandler, M.Q., Williams, N., Wang, P.T., Ruiz, A. (2010). Corrosion relationships as a function of time and surface roughness on a structural AE44 magnesium alloy. *Corros. Sci.* 52 (5), 1635–1648. <https://doi.org/10.1016/j.corsci.2010.01.018>.
- Agarwal, S., Curtin, J., Duffy, B., Jaiswal, S. (2016). Biodegradable magnesium alloys for orthopaedic applications: A review on corrosion, biocompatibility and surface modifications. *Mat. Sci. Eng. C* 68, 948–963. <https://doi.org/10.1016/j.msec.2016.06.020>.
- Aydin, I., Bahcepinar, A.I., Kirman, M., Cipiloğlu, M.A. (2019). HA Coating on Ti6Al7Nb Alloy Using an Electrophoretic Deposition Method and Surface Properties Examination of the Resulting Coatings. *Coatings* 9 (6), 402. <https://doi.org/10.3390/coatings9060402>.
- Bandyopadhyay, A., Espana, F., Balla, V.K., Bose, S., Ohgami, Y., Davies, N.M. (2010). Influence of porosity on mechanical properties and in vivo response of Ti6Al4V implants. *Acta Biomater.* 6 (4), 1640–1648. <https://doi.org/10.1016/j.actbio.2009.11.011>.
- Bartmanski, M., Zielinski, A., Majkowska-Marzec, B., Strugala, G. (2018). Effects of solution composition and electrophoretic deposition voltage on various properties of nanohydroxyapatite coatings on the Ti13Zr13Nb alloy. *Ceram. Int.* 44 (16), 19236–19246. <https://doi.org/10.1016/j.ceramint.2018.07.148>.
- Bogdanovicene, I., Beganskiene, A., Tõnsuaadu, K., Glaser, J., Meyer, H.-J., Kareiva, A. (2006). Calcium hydroxyapatite,  $\text{Ca}_{10}(\text{PO}_4)_6(\text{OH})_2$  ceramics prepared by aqueous sol-gel processing. *Mater. Res. Bull.* 41 (9), 1754–1762. <https://doi.org/10.1016/j.materresbull.2006.02.016>.
- Brandes, E.A., Brook, G.B. (1998). *Smithells Light Metals Handbook*. Eds. Butterworth-Heinemann, Oxford. <https://doi.org/10.1016/B978-075063625-4/50004-1>.
- Brusciotti, F., Snihirova, D.V., Xue, H., Montemor, M.F., Lamaka, S.V., Ferreira, M.G.S. (2013). Hybrid epoxy-silane coatings for improved corrosion protection of Mg alloy. *Corros. Sci.* 67, 82–90. <https://doi.org/10.1016/j.corsci.2012.10.013>.
- Chen, J., Zeng, R.C., Huang, W.J., Zheng, Z.Q., Wang, Z.L., Wang, J. (2008). Characterization and wear resistance of macro-arc oxidation coating on magnesium alloy AZ91 in simulated body fluids. *T. Nonferr. Metal. Soc. China* 18 (1), 361–364. [https://doi.org/10.1016/S1003-6326\(10\)60232-4](https://doi.org/10.1016/S1003-6326(10)60232-4).
- Chen, Y., Yang, Y., Zhang, W., Zhang, T., Wang, F. (2017). Influence of second phase on corrosion performance and formation mechanism of PEO coating on AZ91 Mg alloy. *J. Alloys Compd.* 718, 92–103. <https://doi.org/10.1016/j.jallcom.2017.05.010>.
- Chowdary, S.V., Dumpala, R., Kumar, A., Kondaiah, V.V., Ratna Sunil, B. (2018). Influence of heat treatment on the machinability and corrosion behavior of AZ91 Mg alloy. *J. Magnes. Alloy* 6 (1), 52–58. <https://doi.org/10.1016/j.jma.2017.12.001>.

- Drevet, R., Ben Jaber, N., Fauré, J., Tara, A., Ben Cheikh, A., Benhayoune, H. (2016). Electrophoretic deposition (EPD) of nano-hydroxyapatite coatings with improved mechanical properties on prosthetic Ti6Al4V substrates. *Surf. Coat. Tech.* 301, 94–99. <https://doi.org/10.1016/j.surfcoat.2015.12.058>.
- Dudek, K., Goryczka, T. (2016). Electrophoretic deposition and characterization of thin hydroxyapatite coatings formed on the surface of NiTi shape memory alloy. *Ceram. Int.* 42(16), 19124–19132. <https://doi.org/10.1016/j.ceramint.2016.09.074>.
- Esmaily, M., Mortazavi, N., Svensson, J.E., Halvarsson, M., Jarfors, A.E.W., Wessén, M., Arrabal, R., Johansson, L.G. (2016). On the microstructure and corrosion behavior of AZ91/SiC composites produced by rheocasting. *Mater. Chem. Phys.* 180, 29–37. <https://doi.org/10.1016/j.matchemphys.2016.05.016>.
- Javidi, M., Javadpour, S., Bahrololoom, M.E., Ma, J. (2008). Electrophoretic deposition of natural hydroxyapatite on medical grade 316L stainless steel. *Mat. Sci. Eng. C* 28(8), 1509–1515. <https://doi.org/10.1016/j.msec.2008.04.003>.
- Iqbal, N., Nazir, R., Asif, A., Chaudhry, A.A., Akram, M., Fan, G.Y., Akram, A., Amin, R., Park, S.H., Hussain, R. (2012). Electrophoretic deposition of PVA coated hydroxyapatite on 316L stainless steel. *Curr. Appl. Phys.* 12(3), 755–759. <https://doi.org/10.1016/j.cap.2011.11.003>.
- Ivanova, E.P., Bazaka, K., Crawford, R.J. (2014). *Metallic biomaterials: types and advanced applications*. In *New Functional Biomaterials for Medicine and Healthcare*. Woodhead Publishing, pp. 121–147. <https://doi.org/10.1533/9781782422662.121>.
- Khalili, V., Khalil-Allafi, J., Sengstock, C., Motemani, Y., Paulsen, A., Frenzel, J., Eggeler, G., Köller M. (2016). Characterization of mechanical properties of hydroxyapatite-silicon-multi walled carbon nano tubes composite coatings synthesized by EPD on NiTi alloys for biomedical application. *J. Mech. Behav. Biomed.* 59, 337–352. <https://doi.org/10.1016/j.jmbbm.2016.02.007>.
- Kumar, R.M., Kuntal, K.K., Singh, S., Gupta, P., Bhushan, B., Gopinath, P., Lahiri, D. (2016). Electrophoretic deposition of hydroxyapatite coating on Mg–3Zn alloy for orthopaedic application. *Surf. Coat. Tech.* 287, 82–92. <https://doi.org/10.1016/j.surfcoat.2015.12.086>.
- Kwok, C.T., Wong, P.K., Cheng, F.T., Man, H.C. (2009). Characterization and corrosion behavior of hydroxyapatite coatings on Ti6Al4V fabricated by electrophoretic deposition. *Appl. Surf. Sci.* 255(13–14), 6736–6744. <https://doi.org/10.1016/j.apsusc.2009.02.086>.
- Luo, J., Jia, X., Gu, R., Zhou, P., Huang, Y., Sun, J., Yan, M. (2018). 316L stainless steel manufactured by selective laser melting and its biocompatibility with or without hydroxyapatite coating. *Metals* 8(7), 548. <https://doi.org/10.3390/met8070548>.
- Miranda, G., Sousa, F., Costa, M.M., Bartolomeu, F., Silva, F.S., Carvalho, O. (2019). Surface design using laser technology for Ti6Al4V-hydroxyapatite implants. *Opt. Laser Technol.* 109, 488–495. <https://doi.org/10.1016/j.optlastec.2018.08.034>.
- Morteza, F.R., Shahrabi, T. (2013). Effect of triethanolamine on the electrophoretic deposition of hydroxyapatite nanoparticles in isopropanol. *Ceram. Int.* 39(6), 7007–7013. <https://doi.org/10.1016/j.ceramint.2013.02.038>.
- Morteza, F.R. (2018a). Electrophoretic deposition of hydroxyapatite nanoparticles: effect of suspension composition on the electrochemical potential difference at deposit/suspensions interface. *Mater. Res. Express* 5, 085005. <https://doi.org/10.1088/2053-1591/aad1a2>.
- Morteza, F.R. (2018b). Effect of morphology on the electrophoretic deposition of hydroxyapatite nanoparticles. *J. Alloys Compd.* 741, 211–222. <https://doi.org/10.1016/j.jallcom.2018.01.101>.
- Niu, B., Shi, P., Shanshan, E., Wei, D., Li, Q., Chen, Y. (2016). Preparation and characterization of HA sol-gel coating on MAO coated AZ31 alloy. *Surf. Coat. Tech.* 286, 42–48. <https://doi.org/10.1016/j.surfcoat.2015.11.056>.
- Pang, X., Casagrande, T., Zhitomirsky, I. (2009). Electrophoretic deposition of hydroxyapatite–CaSiO<sub>3</sub>–chitosan composite coatings. *J. Colloid Interf. Sci.* 330(2), 323–329. <https://doi.org/10.1016/j.jcis.2008.10.070>.
- Pasinli, A., Yuksel, M., Celik, E., Sener, S., Tas, A.C. (2010). A new approach in biomimetic synthesis of calcium phosphate coatings using lactic acid-Na lactate buffered body fluid solution. *Acta Biomaterialia* 6(6), 2282–2288. <https://doi.org/10.1016/j.actbio.2009.12.013>.
- Perez, N. (2004). *Electrochemistry and Corrosion Science*. Kluwer Academic Publishers, Boston, New York.
- Rojaei, R., Fathi, M., Raeissi, K. (2013). Controlling the degradation rate of AZ91 magnesium alloy via sol-gel derived nanostructured hydroxyapatite coating. *Mat. Sci. Eng. C* 33(7), 3817–3825. <https://doi.org/10.1016/j.msec.2013.05.014>.
- Sabzi, M., Far, M.S., Dezfouli, M.S. (2018). Characterization of bioactivity behavior and corrosion responses of hydroxyapatite-ZnO nanostructured coating deposited on NiTi shape memory alloy. *Ceram. Int.* 44(17), 21395–21405. <https://doi.org/10.1016/j.ceramint.2018.08.197>.
- Salman, S.A., Kuroda, K., Okido, M. (2013). Preparation and Characterization of Hydroxyapatite Coating on AZ31 Mg Alloy for Implant Applications. *Bioinorg. Chem. Appl.* (6 pages), 175756. <https://doi.org/10.1155/2013/175756>.
- Sahoo, B.N., Panigrahi, S.K. (2016). Synthesis, characterization and mechanical properties of in-situ (TiC-TiB<sub>2</sub>) reinforced magnesium matrix composite. *Mater. Design* 109, 300–313. <https://doi.org/10.1016/j.matdes.2016.07.024>.
- Song, G.-L. (2011). *Corrosion of Magnesium Alloy*. Woodhead Publishing, Cambridge.
- Srekanth, D., Rameshbabu, N. (2012). Development and characterization of MgO/hydroxyapatite composite coating on AZ31 magnesium alloy by plasma electrolytic oxidation coupled with electrophoretic deposition. *Mater. Lett.* 68, 439–442. <https://doi.org/10.1016/j.matlet.2011.11.025>.
- Tahmasebifar, A., Kayhan, S.M., Evis, Z., Tezcaner, A., Çinici, H., Koç, M. (2016). Mechanical, electrochemical and biocompatibility evaluation of AZ91D magnesium alloy as a biomaterial. *J. Alloys Compd.* 687, 906–919. <https://doi.org/10.1016/j.jallcom.2016.05.256>.
- Wang, X.J., Hu, X.S., Liu, W.Q., Du, J.F., Wu, K., Huang, Y.D., Zheng, M.Y. (2017). Ageing behavior of as-cast SiCp/AZ91 Mg matrix composites. *Mat. Sci. Eng. A* 682, 491–500. <https://doi.org/10.1016/j.msea.2016.11.072>.
- Zhang, L., Zhang, J., Chen, C.F., Gu, Y. (2015). Advances in microarc oxidation coated AZ31 Mg alloys for biomedical applications. *Corros. Sci.* 91, 7–28. <https://doi.org/10.1016/j.corsci.2014.11.001>.